Escape rate for nonequilibrium processes dominated by strong non-detailed balance force

Ying Tang, Song Xu, and Ping Ao

Citation: The Journal of Chemical Physics **148**, 064102 (2018); doi: 10.1063/1.5008524
View online: https://doi.org/10.1063/1.5008524
View Table of Contents: http://aip.scitation.org/toc/jcp/148/6
Published by the American Institute of Physics

Escape rate for nonequilibrium processes dominated by strong non-detailed balance force

Ying Tang,[1,a),b)] Song Xu,[2,a),c)] and Ping Ao[3,4,d)]
[1]*Department of Physics and Astronomy, Shanghai Jiao Tong University, Shanghai 200240, China*
[2]*Department of Biomathematics, University of California at Los Angeles, Los Angeles, California 90095-1766, USA*
[3]*Key Laboratory of Systems Biomedicine Ministry of Education, Shanghai Center for Systems Biomedicine, Shanghai Jiao Tong University, Shanghai 200240, China*
[4]*Shanghai Center for Quantitative Life Sciences and Physics Department, Shanghai University, Shanghai 200444, China*

(Received 6 October 2017; accepted 22 January 2018; published online 8 February 2018)

Quantifying the escape rate from a meta-stable state is essential to understand a wide range of dynamical processes. Kramers' classical rate formula is the product of an exponential function of the potential barrier height and a pre-factor related to the friction coefficient. Although many applications of the rate formula focused on the exponential term, the prefactor can have a significant effect on the escape rate in certain parameter regions, such as the overdamped limit and the underdamped limit. There have been continuous interests to understand the effect of non-detailed balance on the escape rate; however, how the prefactor behaves under strong non-detailed balance force remains elusive. In this work, we find that the escape rate formula has a vanishing prefactor with decreasing friction strength under the strong non-detailed balance limit. We both obtain analytical solutions in specific examples and provide a derivation for more general cases. We further verify the result by simulations and propose a testable experimental system of a charged Brownian particle in electromagnetic field. Our study demonstrates that a special care is required to estimate the effect of prefactor on the escape rate when non-detailed balance force dominates. *Published by AIP Publishing.* https://doi.org/10.1063/1.5008524

I. INTRODUCTION

The escape phenomena from a meta-stable state driven by noise serves as a generic model for a variety of dynamical processes in physics,[1–5] chemistry,[6,7] and biology.[8,9] The pioneering work by Kramers[1] provides an analytical formulation on the thermally activated barrier crossing. The results include an exponential function of the potential barrier height, known as the van't Hoff-Arrhenius law,[10,11] and a prefactor related to the friction coefficient. Especially, the prefactor tends to vanish when the friction goes to both zero (underdamped limit) and infinity (overdamped limit). This behavior demonstrates that the prefactor can play a significant role in determining the escape rate, and thus it requires a careful treatment on the prefactor when calculating the escape rate under a certain limit of physical parameters. Besides the dissipation caused by friction, nonequilibrium systems typically shows breakdown of detailed balance condition.[12,13] Quantifying the effect of non-detailed balance on the escape rate will lead to new understandings in a class of escape problems for nonequilibrium systems.

It is a challenge to answer this question. First, the equilibrium Boltzmann-Gibbs distribution given by *a priori* potential function is generally absent.[14] Second, the dynamical trajectories in phase space are governed by a nongradient drift field. The non-detailed balance force may drive trajectories to rotate around the attractor on a nearly closed orbit,[15,16] while noise slowly moves the orbit up and down and finally escapes the potential well. This is in contrast with the case when detailed balance condition holds, where the trajectories stochastically climb up and down the potential barrier without oscillations as illustrated in Fig. 1. A previous study[17] calculated the escape rate under a small non-detailed balance force by treating it as a perturbation. The result shows that non-detailed balance leads to a modification on the prefactor in the rate formula. It remains elusive how the prefactor behaves when such non-detailed balance force is strong and the dynamics cannot be approximated by a perturbation.

In this paper, we study the escape problem for the Langevin dynamics with a strong non-detailed balance. We find that the prefactor in the escape rate formula tends to zero under this limit, whereas directly applying the previous rate formulas[6,17–19] does not give such limiting behavior. For the sake of better demonstration, we study a two-dimensional escape problem, but the analysis is applicable to models of any dimension. We analytically solve the escape rate for specific examples and use simulations to verify the results. We then give a derivation on the escape rate for general two-dimensional Langevin dynamics under the current limit.

The current model can be realized by first taking the zero-mass limit[20,21] and then the strong non-detailed balance limit in a real physical system. This operation is different from directly taking the overdamped limit in a Langevin

[a)]Y. Tang and S. Xu contributed equally to this work.
[b)]jamestang23@gmail.com
[c)]song.xu.ucla@gmail.com
[d)]aoping@sjtu.edu.cn

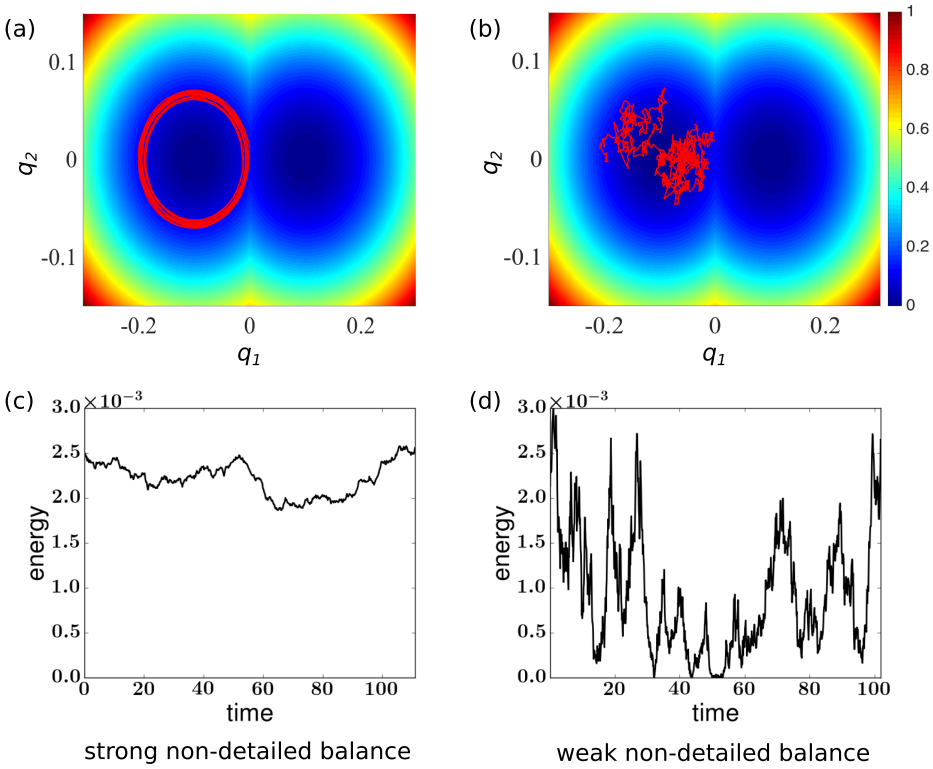

FIG. 1. Double-well potential and escaping trajectories (red) under the strong (a) and weak (b) non-detailed balance limits are displaced. Energy changes along the escaping trajectories for (a) and (b) are shown in (c) and (d), respectively. The weak non-detailed balance model shows much larger energy fluctuation than the strong non-detailed balance model. For visualization purpose, the initial position in (a) was set to $(q_1, q_2) = (-0.2, 0)$ so that the initial energy is close to the escape energy and "escape event" is clearer to observe. Only one position was plotted in every 1000 units of time in (b) so that the trajectory is visible. All the trajectories were recorded until they hit the boundary $q_1 = 0$ for the first time. In [(a) and (c)], $\gamma = 3.4 \times 10^{-4}$, $dt = 10^{-5}$. In [(b) and (d)], $\gamma = 10$, $dt = 0.1$. Other parameters used in both cases are $h = 1/\sqrt{2}$, $\epsilon = 7.5 \times 10^{-4}$, $B_3 = 1$, and $q^* = 0.1$.

equation,[22,23] where the strong non-detailed balance limit could not be achieved afterwards. Indeed, this subtlety in the order of taking the two limits is an obstacle for uncovering the effects of strong non-detailed balance in general escape problems. We show explicitly that the two limits can coexist. Then, in light of Kramers' method on studying the underdamped Langevin dynamics,[1] we transform the coordinates in the position space to the energy-angular coordinate, which enables us to obtain the analytical escape rate. We further propose an experimental system of a charged Brownian particle in magnetic field to test our results.

In Sec. II, we describe the stochastic dynamics, study two examples to demonstrate the result on the escape rate, and then give a general derivation. In Sec. III, we show that computer simulations validate the theoretical result on the escape rate under the strong non-detailed balance limit. Then, we demonstrate the zero-mass limit and propose an experimental protocol to realize the system we studied in Sec. IV. In Sec. V, we compare our result with the previous studies on the escape rate formula and summarize the results. In Appendixes A and B, we describe the transformation of the Fokker-Planck equation to the energy-angular coordinates. We additionally solved the same model as in Example 1 except that the overdamped limit is taken as reference.

II. THEORETICAL FORMULATION AND RESULT

We consider a model of two-dimensional Langevin dynamics under zero-mass limit.[24] A point particle with $\boldsymbol{q} = (q_1, q_2)$ as the state vector is subject to a drift field $\mathbf{f}(\mathbf{q}) = (f_1(\mathbf{q}), f_2(\mathbf{q}))$ and stochastic noise,

$$\dot{\mathbf{q}} = \mathbf{f}(\mathbf{q}) + \boldsymbol{\xi}(t), \tag{1}$$

with $\dot{\mathbf{q}}$ as the time derivative. The Gaussian white noise obeys $\langle \boldsymbol{\xi}(t) \rangle = 0$, and $\langle \boldsymbol{\xi}^T(t)\boldsymbol{\xi}(s) \rangle = 2\epsilon D\delta(t-s)$ with the average taken with respect to the noise distribution and ϵ denoting the Boltzmann constant multiplied by temperature $k_B T$.[13] The diffusion matrix is chosen to be proportional to the identity matrix, $D = bI_2$, where I_2 denotes the two-dimensional identity matrix. For general constant diffusion matrix without singularity, it can be transformed to an identity matrix by coordinate transformation.

For the Langevin equation (1), the corresponding dynamical process for the probability distribution $\rho(\mathbf{q}, t)$ is given by the Fokker-Planck equation,

$$\partial_t \rho(\mathbf{q}, t) = -\sum_{i=1}^{2} \partial_{q_i}[f_i(\mathbf{q})\rho(\mathbf{q}, t)] + \sum_{i,j=1}^{2} \epsilon D_{ij} \partial_{q_i}\partial_{q_j}\rho(\mathbf{q}, t). \tag{2}$$

Note that the diffusion coefficient is constant (addictive noise).

For nonequilibrium systems without detailed balance, the drift field is typically non-gradient: $\mathbf{f}(\mathbf{q}) \neq -D\nabla_{\mathbf{q}}\phi(\mathbf{q})$, where $\phi(\mathbf{q})$ is the scalar potential function. Still, the drift force can also be decomposed as[25,26]

$$\mathbf{f}(\mathbf{q}) = -D\nabla_{\mathbf{q}}\phi(\mathbf{q}) - Q\nabla_{\mathbf{q}}\phi(\mathbf{q}), \tag{3}$$

where Q is an antisymmetric matrix corresponding to the breakdown of the detailed-balance condition. The diffusion coefficient D as the prefactor of the gradient term is imposed by the fluctuation-dissipation theorem of second kind.[27]

We consider the case with constant matrices D and Q, and thus there is no ambiguity on choosing the integration method on Eq. (1), e.g., the Ito-Stratonovich dilemma.[13,28,29] Then, by using any stochastic integration, the Fokker-Planck equation (2) is rewritten as[25]

$$\partial_t \rho(\mathbf{q},t) = \sum_{i,j=1}^{2} [D_{ij} + Q_{ij}]\partial_{q_i}\{[\partial_{q_j}\phi(\mathbf{q}) + \epsilon\partial_{q_j}]\rho(\mathbf{q},t)\}. \quad (4)$$

In order to clearly demonstrate the definition on the strong non-detailed balance limit, we consider the case with $D = bI_2$. We also choose the antisymmetric matrix $Q = a\Omega_1$, where a is a constant and Ω_1 is a two-dimensional symplectic matrix. Then, Eq. (4) can be simplified as

$$\partial_t \rho(\mathbf{q},t) = \sum_{i,j=1}^{2} Q_{ij}[\partial_{q_j}\phi(\mathbf{q})]\partial_{q_i}\rho(\mathbf{q},t) + b\sum_{i=1}^{2}\partial_{q_i} \times \{[\partial_{q_i}\phi(\mathbf{q})]\rho(\mathbf{q},t) + \epsilon\partial_{q_i}\rho(\mathbf{q},t)\}. \quad (5)$$

The strong non-detailed balance limit is realized as $b \gg a$, which corresponds to that the magnitude of non-detailed balance force is much larger than the detailed balance part.

For more general cases, the way of defining a non-strong detailed balance limit here can be extended. It should be defined as that the magnitude of the antisymmetric part $Q\nabla_{\mathbf{q}}\phi(\mathbf{q})$ in Eq. (3) is larger than that of the symmetric part $D\nabla_{\mathbf{q}}\phi(\mathbf{q})$, with the latter negligible. This can be realized by using a certain norm of matrices to quantify their relative magnitude. In the following, we give the escape rate under the strong non-detailed balance limit in specific examples.

A. First example

We first provide an example where we calculate analytically the rate formula under the strong non-detailed balance limit. This example has a piecewise double-well potential: $\phi(q_1,q_2) = h^2(q_1+q^*)^2/2 + q_2^2/2$, when $q_1 \le 0$, and $\phi(q_1,q_2) = h^2(q_1-q^*)^2/2 + q_2^2/2$, when $q_1 \ge 0$. The parameter h is constant denoting the "stiffness" of potential along the q_1 direction. The two potential wells W_1 and W_2 are $(-q^*, 0)$ and $(q^*, 0)$ with $q^* > 0$. The potential function is harmonic around each well and is symmetric about the q_2-axis. A similar potential has been studied by Kramers for the escape problem under a large friction limit in one dimension.[1] As an example, given the diffusion matrix $D = bI_2$, the drift field in Eq. (1) is specified as

$$\begin{cases} f_1 = -b\partial_{q_1}\phi - aq_2, \\ f_2 = -b\partial_{q_2}\phi + ah^2(q_1+q^*). \end{cases} \quad (6)$$

An experimental realization of the system is described below [cf. Eq. (20)], where $b \to 0$ corresponds to the strong non-detailed balance limit.

Motivated by Kramers' idea for studying an one-dimensional particle in the momentum-position space in the case of small viscosity,[1] we describe the energy coordinate for the two-dimensional equations (1)–(6). When the noise variation is small, i.e., in the limit $b \to 0$, the Brownian force only leads to a small perturbation on the energy of oscillation. According to the fluctuation-dissipation theorem, the effect of gradient drift field $-D\nabla_{\mathbf{q}}\phi(\mathbf{q})$ in Eq. (3) is also small. Therefore, the particle dominately performs an oscillatory motion under the non-detailed balance drift field. The energy gradually changes with the angles of oscillation as the slow variable. Then, we introduce the energy coordinate system (E, θ) with $q_1 = \sqrt{2E/h^2}\cos\theta - q^*$, $q_2 = \sqrt{2E}\sin\theta$. Note that $\phi(q_1, q_2) = E$ inside the left well.

Next, we consider the average in the ring-shaped energy surface area with $E \le \phi \le E + dE$. We define the average on this energy surface, $\overline{A} \doteq \int_{E\le\phi\le E+dE} A dS / \int_{E\le\phi\le E+dE} dS$. When the particle moves in the left well, we get $\overline{\partial_{q_1}^2\phi + \partial_{q_2}^2\phi} = (h^2+1)$, $\overline{(\partial_{q_1}\phi)^2 + (\partial_{q_2}\phi)^2} = (h^2+1)E$. Then, we apply the transformation for the moment function in the Fokker-Planck equation when changing the coordinate[30] as also detailed in Appendix A and take the average over the energy surface to Eq. (2). The transformed moment functions after taking average are $\bar{f}_1 = (h^2+1)(\epsilon - E)$, $\bar{D}_{11} = (h^2+1)E$. Therefore, the Fokker-Planck equation becomes

$$\partial_t \bar{\rho}(E,t) = b(h^2+1)\partial_E[E(\bar{\rho} + \epsilon\partial_E\bar{\rho})]. \quad (7)$$

The current density for the steady state is

$$w = -b(h^2+1)\epsilon E e^{-E/\epsilon}\partial_E(\bar{\rho}e^{E/\epsilon}). \quad (8)$$

We consider the escape problem that the particle starting around the well W_1 escapes out the well to another W_2 through the saddle point S. Although escaping through any point on the q_2-axis is possible, all other points have higher potential energy than the saddle $q_1 = q_2 = 0$. Our choice is valid as argued by Kramers[1] that points which are "shuttled" up to an energy larger than the saddle will immediately travel to the other potential well. We rewrite Eq. (8) as $we^{E/\epsilon}/E = -b(h^2+1)\epsilon\partial_E(\bar{\rho}e^{E/\epsilon})$ and integrate it between two positions W_1 and S in terms of the energy coordinate E, giving $w = b(h^2+1)\epsilon[(\bar{\rho}e^{E/\epsilon})_{nearW_1} - (\bar{\rho}e^{E/\epsilon})_S]/[\int_{nearW_1}^{S} e^{E/\epsilon}/EdE]$. We assume that particles leaving at saddle point S will practically never re-enter the well region around W_1, which leads to that $(\bar{\rho}e^{E/\epsilon})_S = 0$. Denoting $\bar{\rho}_{W_1} \doteq (\bar{\rho}e^{E/\epsilon})_{nearW_1}$, we get $w \approx b(h^2+1)\epsilon\bar{\rho}_{W_1}(\int_{\epsilon}^{S} e^{E/\epsilon}/EdE)^{-1}$, where we have taken the energy value near W_1 as ϵ by assuming that the energy near W_1 is only due to fluctuation of noise. Since the main contribution of the integral is from energy values that differ from ΔE by a quantity with the same order of magnitude as ϵ, we may take the energy value at position S corresponding to energy difference ΔE between positions S and W_1, $\int_{\epsilon}^{\Delta E} e^{E/\epsilon}/EdE \approx (1/\Delta E)e^{\Delta E/\epsilon}\int_0^{+\infty} e^{-(\Delta E - E)/\epsilon}d(\Delta E - E) = (\epsilon/\Delta E)e^{\Delta E/\epsilon}$, where we have extended the upper limit of integration from $\Delta E - \epsilon \approx \Delta E$ to $+\infty$ as a larger value does not contribute to the integral.

The number of particles assembled near W_1 is $n_{W_1} \approx \int_0^{+\infty} dE\bar{\rho}_{W_1}e^{-E/\epsilon} \approx \bar{\rho}_{W_1}\epsilon$. Then, the escape rate formula is obtained from the current divided by the particle density,

$$r = \frac{w}{n_{W_1}} \approx b\frac{(h^2+1)\Delta E}{\epsilon}e^{-\Delta E/\epsilon}. \quad (9)$$

Note that when $b \to 0$, the escape rate also tends to zero ($r \to 0$). It implies that when the detailed balance part is finite, the escape time goes to infinite as the strength of the diffusion coefficient (noise variation) converges to zero in Eq. (1).

We test the limiting behavior of rate formula Eq. (9) by simulations. In Fig. 2, the match between the numerical simulation and theoretical prediction becomes better and eventually coincide when the friction coefficient $\gamma \to \infty$ or the magnetic intensity $B_3 \to 0$, corresponding to $b \to 0$ in Eq. (9). Besides, we find that the simulation time gets longer when $b \to 0$, which indicates that the most probable escape path is longer.

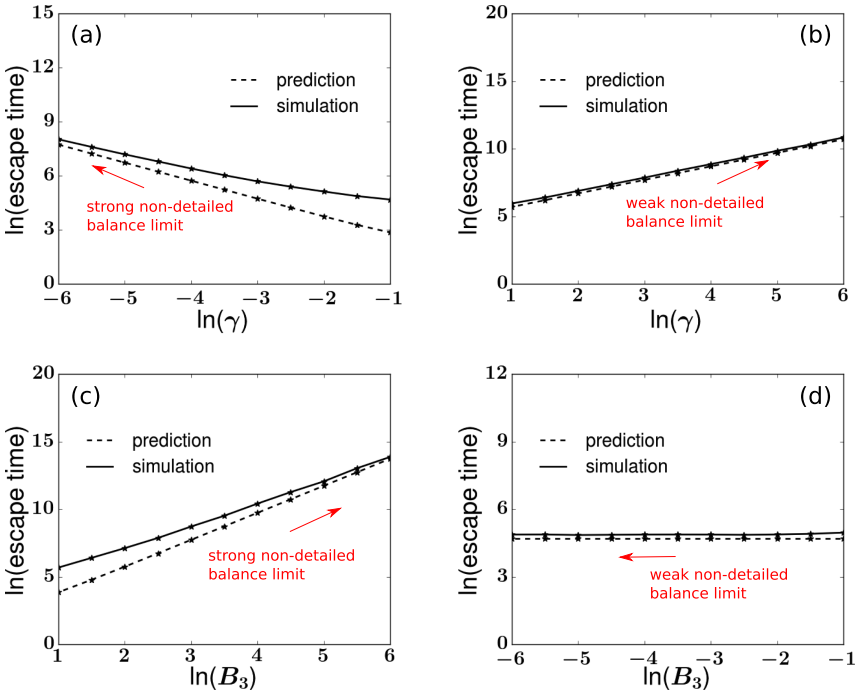

FIG. 2. Simulated (solid) and analytical (dashed) escape times with varyingfriction coefficient γ [(a) and (b)] or varying magnetic intensity B_3 [(c) and (d)] under the strong [(a) and (c)] and weak [(b) and (d)] non-detailed balance limits. A number of 10 000 simulations were performed for each γ, and the average of the 10 000 escape times is plotted. B_3 is fixed to 1 in [(a) and (b)] while γ is fixed to 1 in [(c) and (d)]. Other parameters used in all cases are $\epsilon = 7.5 \times 10^{-4}$, $dt = 3.3 \times 10^{-6} + 10^{-3} \sin(\frac{\pi}{4} |\frac{q_1}{q^*}|)$, $h = 1/\sqrt{2}$, and $q^* = 0.1$.

In Fig. 3, we illustrate how the most probable escape path depends on the parameters, which is a salient feature of systems without detailed balance. This supports the observation by Landauer that the escape rate is dependent on kinetics along the path connecting steady states when detailed balance breaks down.[31]

B. Second example

As another example, we study the system

$$\begin{cases} \dot{q}_1 = -a\partial_{q_2}\phi, \\ \dot{q}_2 = a\partial_{q_1}\phi - b\partial_{q_2}\phi + \xi(t), \end{cases} \tag{10}$$

with $\langle \xi(t) \rangle = 0$ and $\langle \xi^T(t)\xi(s) \rangle = 2\epsilon b\delta(t-s)$.

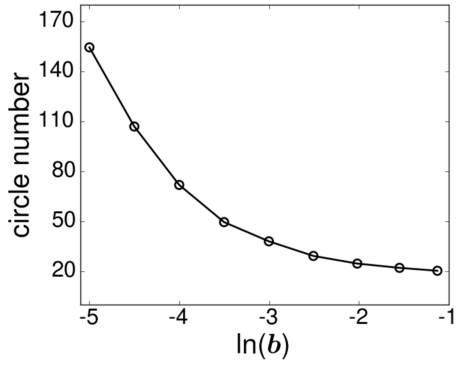

FIG. 3. Simulation shows that the characteristic of the most probable escape path, e.g., the number of "circles" in Fig. 1(a), depends on the parameter b corresponding to the relative magnitude between non-detailed balance and detailed balance parts. Under the strong non-detailed balance limit, e.g., $b \to 0$, the particle would undergo a number of "circles" around the valley state $(-0.1, 0)$ before finally escaping as shown in Fig. 1(a). The expected number of circles increases with relatively larger non-detailed balance force as b becomes smaller. The statistics here are obtained by averaging over 10 000 simulated trajectories for each b.

This system can be exactly mapped to the phase space with the momentum coordinate $p \to q_1$ and the position coordinate $q \to q_2$ in Ref. 1 for the underdamped case. Therefore, the techniques used there can be directly applied here to get the rate formula. We emphasize that although the techniques are the same, the problem considered here is a totally different case: the present equation (10) is a Langevin system under the zero mass limit, whereas the mapping to the energy-angular coordinate in Ref. 1 is for the case under the underdamped limit.

For this system, we can study the escape problem under general smooth potential functions. We consider a potential function with double well in the q_1 direction,

$$\phi(q_1, q_2) = \frac{1}{2}q_2^2 - \frac{1}{2}q_1^2 + \frac{1}{4}q_1^4. \tag{11}$$

By introducing the energy coordinate $E \doteq \phi(q_1, q_2)$, we obtain the Fokker-Planck equation for Eq. (10) as

$$\begin{aligned} \partial_t \bar{\rho} &= b\partial_{q_2}[(\partial_{q_2}E)(\bar{\rho} + \epsilon\partial_E\bar{\rho})] \\ &= b\partial_{q_2}[q_2(\bar{\rho} + \epsilon\partial_E\bar{\rho})] \\ &= b[(\bar{\rho} + \partial_E\bar{\rho}) + q_2^2\partial_E(\bar{\rho} + \epsilon\partial_E\bar{\rho})]. \end{aligned} \tag{12}$$

Denote the area inside a ring-shaped energy by $I(E) = \oint q_2 dq_1$ and the fraction of the ensemble lying inside this ring-shaped area dI by $\overline{q_2}dI$. The frequency ω is given by $\omega = dE/dI$ and we have $\overline{q_2^2} = I\omega$. After taking the average over the energy surface, i.e., for any quantity A the average $\overline{A} \doteq \int_{E\le\phi\le E+dE} A dS / \int_{E\le\phi\le E+dE} dS$, we obtain the Fokker-Planck equation as

$$\begin{aligned} \partial_t \bar{\rho} &= b[(\bar{\rho} + \epsilon\partial_E\bar{\rho}) + \overline{q_2^2}\partial_E(\bar{\rho} + \epsilon\partial_E\bar{\rho})] \\ &= b[(1 + I\omega\partial_E)(\bar{\rho} + \epsilon\partial_E\bar{\rho})] \\ &= b\partial_I(\bar{\rho}I + \epsilon I\partial_I\bar{\rho}), \end{aligned} \tag{13}$$

which has the same form of the Fokker-Planck equation as that in Ref. 1. Therefore, we directly apply the result here and get

the escape rate,

$$r \approx b\frac{\Delta E}{\epsilon}e^{-\Delta E/\epsilon}, \tag{14}$$

where ΔE is the potential difference between the stable point W_1 and the saddle point S. This result is consistent with that obtained for Eq. (6) under the strong non-detailed balance limit.

C. General case

We provide a derivation to reach the rate formula for general equation (1) under the limit of $b \to 0$. Though we consider a two-dimensional case here, the method can be applied to higher-dimensional systems under the same limit. Following the procedure in the above example, we change the coordinates to the energy coordinate E and the angular coordinate θ. We first make coordinate transformation on the corresponding Fokker-Planck equation (2), with the detailed derivation given in Appendix A. Then, conduct an average along a ring-shaped energy surface by integrating θ on the surface. The terms with ∂_θ are equal to zero due to periodicity on θ. We thus obtain a Fokker-Planck equation,

$$\partial_t \bar{\rho}(E,t) = b(-\partial_E \bar{f}_1 + \epsilon\partial_E^2 \bar{D}_{11})\bar{\rho}(E,t), \tag{15}$$

where for any quantitative A the symbol $\bar{A} \doteq \int_{E\le\phi\le E+dE} A dS / \int_{E\le\phi\le E+dE} dS$ denotes the average density over the chosen energy surface. The transformed moment functions after average are $\bar{f}_1 = -(\partial_{q_1}E)^2 - (\partial_{q_2}E)^2 + \epsilon(\partial_{q_1}^2 E + \partial_{q_2}^2 E)$ and $\bar{D}_{11} = (\partial_{q_1}E)^2 + (\partial_{q_2}E)^2$. Note that Eq. (15) is of the same form as the Fokker-Planck equation under the energy-diffusion approximation in Ref. 2.

The steady state current is

$$w = b(\bar{f}_1 - \epsilon\partial_E \bar{D}_{11})\bar{\rho}(E,t). \tag{16}$$

Then, we introduce $\int^{E''}[\bar{f}(E')/\bar{D}_{11}(E')]dE' = -\phi_E(E'')$ to define a potential function in energy coordinate ϕ_E with $\Delta\phi_E \approx \phi_E(E_S) - \phi_E(0)$. By applying boundary condition $\rho_{ss}(E_S) = 0$, we get the reduced steady state solution,

$$\rho_{ss}(E) = w/[b\epsilon\bar{D}_{11}(E)]\exp[-\phi_E(E)/\epsilon] \times \int_E^{E_S}\exp[\phi_E(E'')/\epsilon]dE''. \tag{17}$$

The particle density around the well W_1 is $n_{W_1} \doteq \int_0^{E_S}\rho_{ss}(E)dE$. Then, the escape rate by dividing the current divided with the particle density is obtained,

$$\begin{aligned} r \doteq w/n_{W_1} &= b\Big\{\int_0^{E_S}\frac{1}{\epsilon\bar{D}_{11}(E)}\exp\Big[\int^{E}\frac{\bar{f}(E')}{\epsilon\bar{D}_{11}(E')}dE'\Big]\int_E^{E_S}\exp\Big[-\int^{E''}\frac{\bar{f}(E')}{\epsilon\bar{D}_{11}(E')}dE'\Big]dE''dE\Big\}^{-1} \\ &= b\Big\{\int_0^{E_S}\frac{1}{\epsilon\bar{D}_{11}(E)}\exp[-\phi_E(E)/\epsilon]\int_E^{E_S}\exp[\phi_E(E'')/\epsilon]dE''dE\Big\}^{-1} \\ &\approx b\bar{D}_{11}(E^*)\Big\{\int_0^{E_S}\exp[-\phi_E(E)/\epsilon]\exp(-\Delta\phi_E/\epsilon)dE\Big\}^{-1} \\ &\approx (b\bar{D}_{11}(E^*)/\epsilon)\exp(-\Delta\phi_E/\epsilon), \end{aligned} \tag{18}$$

where we have used the definition on the potential function. From the third line to the fourth line, the main contribution of the integral $\exp[-\phi_E(E)/\epsilon]\int_E^{E_S}\exp[\phi_E(E'')/\epsilon]dE''$ comes from $E \approx 0$, and thus we have applied the approximation $\int_E^{E_S}\exp[\phi_E(E'')/\epsilon]dE'' \approx \int_0^{E_S}\exp[\phi_E(E'')/\epsilon]dE'' \approx \exp(\Delta\phi_E/\epsilon)/\epsilon$. Besides, we have approximated the diffusion coefficient as $\bar{D}_{11}(E^*)$ with $E^* \in (0, E_S]$. When $b \to 0$, the transition rate $r \to 0$. This is consistent with the above analytical result obtained in the two examples.

III. SIMULATION DETAILS

We used Euler's method to simulate Eqs. (6). Ten-thousand tests were run for each parameter set with initial condition $q_1(t_0) = q^* = -0.1$. Each simulation keeps running until $q_1(t_{\mathrm{FPT}}) \ge 0$ for the first time at some t_{FPT}, which denotes the first passage time (FPT). The mean FPT (MFPT) is then calculated from the 10 000 FPTs. Note that in the case of weak non-detailed balance (overdamped limit), the MFPT is multiplied by 2 before comparing to the analytical escape time since a particle will quickly fall into a local stable state after crossing the separatrix $q_1 = 0$ and "the probability of crossing the separatrix in either direction equals one half."[2] In the case of strong non-detailed balance, however, the particle will stay relatively stable on the equi-potential surface and frequently cross the separatrix. The steady escape flow is immediately established after the first passage and there is no need to multiply a factor 2.

In the simulations, the escape time results are found to be very sensitive to the value of dt as $\gamma \to 0$, which is possibly caused by the sensitivity of the barrier-crossing behaviors near the boundary $q_1 = 0$. We choose an adaptive step size,

$$\mathrm{d}t = 10^{-6} + 10^{-3} * \sin\left(\frac{\pi}{2}\cdot\left|\frac{q_1}{0.2}\right|\right). \tag{19}$$

As a result, when the particle is close to the boundary, the time step is as small as 10^{-6}. When it is farther away, the time step becomes as large as 10^{-3}.

IV. EXPERIMENTAL REALIZATION

We consider the system of a charged Brownian particle moving along a two-dimensional potential energy surface with the presence of a magnetic field.[12,32,33] The forces acted on the particle include the friction force, the Lorentz force due to the magnetic field, the potential gradient, and the noise. According

to Newton's 2nd law, the dynamical equation is given by

$$m\ddot{\mathbf{q}} = -\gamma\dot{\mathbf{q}} + e\mathbf{B}\times\dot{\mathbf{q}} - \nabla_{\mathbf{q}}\phi(\mathbf{q}) + \zeta(t), \tag{20}$$

where the constants γ, m, and e denote, respectively, the friction coefficient, mass, and charge of the particle. The Lorentz force is $e\mathbf{B}\times\dot{\mathbf{q}}$, and $\phi(\mathbf{q})$ corresponds to the electrostatic potential. The Gaussian white noise obeys $\langle\zeta(t)\rangle = 0$ and $\langle\zeta^T(t)\zeta(s)\rangle = 2\epsilon S\delta(t-s)$. The friction matrix is chosen to be proportional to an identity matrix, $S = \gamma I_2$. The noise correlation measured by the friction coefficient is imposed by the fluctuation-dissipation theorem of the first kind.[27]

In the zero-mass limit $m \to 0$, Eq. (20) becomes

$$\gamma\dot{\mathbf{q}} - e\mathbf{B}\times\dot{\mathbf{q}} = -\nabla_{\mathbf{q}}\phi(\mathbf{q}) + \zeta(t). \tag{21}$$

As an example of theoretical and experimental implementation of such limits, we refer interested readers to Refs. 20 and 34. We then proceed to rewrite the term of Lorentz force as $e\mathbf{B}\times\dot{\mathbf{q}} = A\dot{\mathbf{q}}$, where A is an antisymmetric matrix. This term can induce a circular current, indicating the breakdown of detailed balance.[12]

The conservation of the Lorentz force also implies that the non-detailed balance condition does not necessarily imply dissipation of the system. The presence of the Lorentz force can induce a circular current, indicating the breakdown of detailed balance.

We specify the magnetic field to be perpendicular to the plane of the particle's trajectory by choosing $e\mathbf{B} \doteq (B_1, B_2, B_3)$ with $B_1 = B_2 = 0$. By introducing the coefficient $b \doteq \gamma/(\gamma^2 + B_3^2)$, $a \doteq -B_3/(\gamma^2 + B_3^2)$, Eq. (21) becomes the example given by Eqs. (1)–(6). Then, the result Eq. (9) demonstrates that for the system of a charged Brownian particle with a finite magnetic field under the zero mass limit in Eq. (21), the escape time is infinite when the friction goes to zero, which is consistent with the physical situation that the particle only under Lorentz force will oscillate with conserved energy.

Next, we propose an experimental scheme for the case discussed in Sec. II. Realizing the limit of $b \to 0$ in Eqs. (1)–(6) requires $m/t_s \ll \gamma \ll B_3$, which leads to $b \approx \gamma/B_3^2$, $a \approx -1/B_3$. We consider a Brownian particle moving in an air chamber. First, as the density of oxygen is 1.429 kg/m^3, we can use a particle with mass density $\rho = 1.5$ kg/m^3. If we choose particle size $R = 10^{-4}$ m, the particle's mass is $m = \rho(4/3)\pi R^3 \approx 6.3 \times 10^{-12}$ kg. Second, the viscosity of air is 1.81×10^{-5} Pa s, and thus the friction coefficient $\gamma \approx 6\pi\eta R = 2.8 \times 10^{-8}$ kg/s. Third, if we take surface charge density $\sigma = 0.5$ C/m^2,[35,36] the total charge of the particle is $e = 4\pi R^2\sigma \approx 6.3 \times 10^{-8}$ C. If adding the external magnetic field $B = 10T$, which is achievable based on the current laboratory condition, $B_3 = eB = 6.3 \times 10^{-7}$ kg/s. Fourth, we take the sampling time to be $t_s \leq 10$ ms as in the experiment.[34] Therefore, during sampling, the particle has already relaxed to equilibrium and is effectively subject to zero total force, which leads an effective mass of zero.[24] As a result, the condition $m/t_s \ll \gamma \ll B_3$ is satisfied. Since B_3 is an order of magnitude larger than γ, a is also larger than b in Eqs. (1)–(6), which corresponds to taking the limit of $b \to 0$. Larger magnetic field can improve realizing the limit, which is the case used in our computer simulations.

V. DISCUSSION

The construction of the Langevin model above depends crucially on the order of taking the two limits. We first take the zero mass limit and then the strong non-detailed balance limit. The zero-mass limit has been studied with mathematical rigor.[20,21,37,38] It originates from a treatment on reducing the $2N$-dimensional Klein-Kramers equation to a N-dimensional Fokker-Planck equation,[20] where parameters of friction and non-detailed balance are finite. If taking the overdamped limit first, one implicitly chooses friction to be infinity. Thus, one cannot generally change the order of taking the two limits, except for the one-dimensional case.[21] In this manuscript, we have provided an experimental scheme to realize the zero mass limit.

Besides the experimental realization proposed above, models under the strong non-detailed balance limit have been studied in the context of magnetic moment of a single-domain ferromagnetic particle by the Langevin equation in Gilbert's form.[39,40] Both their experimental and theoretical estimates yield small values of friction coefficient.[41,42] They also found that the rate formula goes to zero when dissipation becomes small, which is consistent with the present result. Compared with their studies directly starting from a Langevin dynamics without mass, ours is reached by a careful treatment of ordering the limits of zero mass and strong non-detailed balance in the original Langevin dynamics. To our knowledge, the necessity of first taking the zero mass limit is for the first time articulated. The procedure will be useful for classifying the role of non-detailed balance on escape phenomena for general stochastic dynamics. Besides, here we investigate the effect of non-detailed balance on the escape rate for nonequilibrium systems, which is different from these previous studies focusing on magnetic moment.

For the general Langevin dynamics equation (1), a potential function governing the dynamics can be constructed[25] through the decomposition Eq. (3) given in Appendix A. Based on the potential function constructed and the decomposition, we can proceed to derive the rate formula for nonequilibrium systems without detailed balance, which we have achieved under the strong non-detailed balance limit. Instead, the WKB approximation[18,43] relies on the existence of quasi-stationary spatial distribution $\rho(\mathbf{q}, t)$.[44] It only applies to one-dimensional nonequilibrium system and higher-dimensional system reducible to one-dimension or have detailed balance (see p. 301 in Ref. 2). However, this is not the case in the current two-dimensional nonequilibrium system without detailed balance.

Below, we compare our results with the previous generalizations on Kramers' rate formula. We demonstrate that for our example Eq. (6) the previous formulas for the overdamped case could not give the infinite escape time under the limit of $\gamma \to 0$.

1. The Eyring formula for the first mean passage time was obtained in Ref. 6,

$$\tau \propto \frac{2\pi}{\lambda_+^*}\sqrt{\frac{|\det Hess\phi(\mathbf{q}_S)|}{\det Hess\phi(\mathbf{q}_1)}}\exp(\Delta\phi/\epsilon), \tag{22}$$

where *Hess* denotes the Hessian matrix of the potential function at different positions and $-\lambda_+^*$ is the negative eigenvalue of the Hessian matrix at the saddle point S.

For our example, Eq. (6), in the left potential well, the Hessian matrix is

$$Hess\phi = \begin{pmatrix} h^2 & 0 \\ 0 & 1 \end{pmatrix}. \tag{23}$$

It is impossible to get the Hessian matrix at the saddle point where the potential function is continuous but not differentiable. Even so, the prefactor in Eq. (22) is just related to the potential function and does not depend on the friction constant. Therefore, it could not produce the asymptotic behavior that the escape rate goes to zero under the strong non-detailed balance limit.

2. A generalized Eyring formula was provided in Ref. 18,

$$\tau \propto \frac{2\pi}{\lambda_+^*}\sqrt{\frac{|\det Hess\phi(\mathbf{q}_S)|}{\det Hess\phi(\mathbf{q}_1)}}\exp\left(\int_{-\infty}^{+\infty} F(\rho_t)dt\right) \times \exp(\Delta\phi/\epsilon), \tag{24}$$

where the correction term $\exp\left(\int_{-\infty}^{+\infty} F(\rho_t)dt\right)$ with respect to Eq. (22) involves the integral of the function F along the most probable path $(\mathbf{q}_t)_{t\in\mathcal{R}}$ (see the detailed formula in Ref. 18). Similarly, this generalized formula still cannot give a prefactor, which leads to zero escape rate when friction goes to zero.

3. In Ref. 17, the authors treated the breakdown of detailed balance as a perturbation and therefore their rate formula does not become zero when the friction goes small. Specifically, Eq. (30) in their result is

$$\dot{K}/K = -u_1 - D_{q_2}f_2, \tag{25}$$

and for our example $u_1 = -b/m$, $D_{q_2} = b$. Then,

$$\dot{f}_2 = -2D_{q_2}f_2^2 - 2u_1f_2 + 2v_0v_2/D_{q_1} = -2bf_2^2 + 2(b/m)f_2, \tag{26}$$

with $v_0 = m\omega^2$ and $v_2 = 0$. Thus, their formula about the modification on the prefactor cannot give zero escape rate under the strong non-detailed balance limit.

4. Besides, directly applying the results in Ref. 19, i.e., Eqs. (3.37) and (4.13) under the strong non-detailed balance limit, cannot produce that the escape rate $r \to 0$.

5. Furthermore, a series of previous work studied the escape problem with detailed balance condition violated. For example, the distribution of the exit position was investigated in Ref. 45 with employing the construction on quasi-potential. Also, the studies in Refs. 46 and 47 focus on the optimal escape path and the prehistory probability distribution of the escape paths. Besides, the mean first passage time was calculated in Ref. 48 by using the WKB approximation and solving the Hamiltonian-Jacobi equation to get the steady state distribution. Finally, a prefactor depending on the noise strength was obtained in Ref. 49.

   We note that there are two main differences between these studies and ours. First, our result gives an escape rate formula with a prefactor converging to zero under the strong non-detailed balance limit, and this prefactor explicitly depends on the physical parameters of friction and magnetic field. However, the previous studies mentioned above do not generate a prefactor with the similar property. Second, we reach the rate formula by employing a decomposition Eq. (3) on the dynamics. The potential function constructed through the decomposition makes it possible to directly apply the energy-diffusion method to such strong non-detailed balance systems. It leads to a clear-cut classification on the role of non-detailed balance force and detailed balance part to the escape rate. On the other hand, the previous studies mainly use the WKB approximation to get the potential function, which may not enable to define the strong non-detailed balance limit. Besides, we have demonstrated that the equivalence between the quasi-potential and the potential function constructed here achieves only in the small noise limit.[50,51]

VI. CONCLUSION

In conclusion, we have shown how the escape rate can be calculated for the stochastic dynamical system dominated by non-detailed balance force. The resulted rate formula has a prefactor that approaches zero under the strong non-detailed balance limit. The Langevin description of such a process can be obtained by first taking the zero-mass limit and then the strong non-detailed balance limit of a realizable physical model. We have also provided an experimental implementation of this model in an electromagnetic system. Our study serves as a first step towards investigating the escape problem beyond a small non-detailed balance limit and can motivate further studies on the escape rate for nonequilibrium systems without detailed balance.

ACKNOWLEDGMENTS

We thank Nigel Goldenfeld for the discussion. This work is supported in part by the National 973 Project No. 2010CB529200 and by the Natural Science Foundation of China Project Nos. NSFC61073087 and NSFC91029738.

APPENDIX A: FOKKER-PLANCK EQUATION IN THE ENERGY-ANGULAR SPACE

We describe here the coordinate transformation in two-dimensional systems here as an example. For the stochastic dynamics under the same limit, the method can be applied to high dimension without loss of generality. We first introduce the energy coordinate system and perform coordinate transformation on the Fokker-Planck equation. Specifically, $E = \phi(q_1, q_2)$ and $\theta = \theta(q_1, q_2)$ where E denoting the potential energy value is the energy coordinate and θ is the angular coordinate. The coordinate transformation for the Fokker-Planck equation is given by Ref. 30. For a two-dimensional Fokker-Planck equation (2), the transformed Fokker-Planck equation is

$$\partial_t\tilde{\rho}(\tilde{q}_1, \tilde{q}_2, t) = \Big[-\sum_k \partial_{\tilde{q}_k}\tilde{f}_k + \sum_{k,r=1}^{2} \epsilon\partial_{\tilde{q}_k}\partial_{\tilde{q}_r}\tilde{D}_{kr}\Big]\tilde{\rho}(\tilde{q}_1, \tilde{q}_2, t), \tag{A1}$$

with the transformation on the moment functions

$$\tilde{f}_k = \frac{\partial \tilde{q}_k}{\partial q_i} f_i + \frac{\partial^2 \tilde{q}_k}{\partial q_i \partial q_j} Dij, \tag{A2}$$

$$\tilde{D}_{kr} = \frac{\partial \tilde{q}_k}{\partial q_i} \frac{\partial \tilde{q}_r}{\partial q_j} Dij, \tag{A3}$$

$$\tilde{\rho} = J\rho. \tag{A4}$$

In the original coordinate system, the moment functions are

$$f_1 = -\partial_{q_1} E, \quad f_2 = -\partial_{q_2} E, \quad \mathcal{B} = I_2. \tag{A5}$$

Then, we get the transformed moment functions

$$\tilde{f}_1 = -(\partial_{q_1} E)^2 - (\partial_{q_2} E)^2 + \epsilon(\partial_{q_1}^2 E + \partial_{q_2}^2 E), \tag{A6}$$

$$\tilde{f}_2 = -\partial_{q_1}\theta\partial_{q_1} E - \partial_{q_2}\theta\partial_{q_2} E + \epsilon(\theta_{xx} + \theta_{yy}), \tag{A7}$$

$$\begin{aligned} \tilde{D}_{11} &= [(\partial_{q_1} E)^2 + (\partial_{q_2} E)^2], \\ \tilde{D}_{12} &= (\partial_{q_1} E \partial_{q_1}\theta + \partial_{q_2} E \partial_{q_2}\theta) = \tilde{D}_{21}, \\ \tilde{D}_{22} &= (\partial_{q_1}\theta^2 + \partial_{q_2}\theta^2), \end{aligned} \tag{A8}$$

$$\tilde{\rho} \doteq J\rho = \frac{1}{\partial_{q_1} E \partial_{q_2}\theta - \partial_{q_2} E \partial_{q_1}\theta}\rho. \tag{A9}$$

Therefore, Eq. (5) is transformed to be

$$\begin{aligned} \partial_t \tilde{\rho}(E,\theta,t) = &-a\partial_\theta J^{-1}\tilde{\rho}(E,\theta,t) + b\Big[-\partial_E \tilde{f}_1(E,\theta) \\ &- \partial_\theta \tilde{f}_2(E,\theta) + \partial_E^2 \tilde{D}_{11}(E,\theta) + 2\partial_E\partial_\theta \tilde{D}_{12}(E,\theta) \\ &+ \partial_\theta^2 \tilde{D}_{22}(E,\theta)\Big]\tilde{\rho}(E,\theta,t). \end{aligned} \tag{A10}$$

We next conduct an average procedure similar to that in Ref. 1. We integrate θ on a closed equal energy surface, the terms with ∂_θ equal to zero due to periodicity on θ. We thus obtain the Fokker-Planck equation (15).

APPENDIX B: OVERDAMPED LIMIT FOR THE FIRST EXAMPLE

In order to verify that the simulation can successfully match the theory under the overdamped limit, we also study Eq. (6) in this limit by choosing $a = 0$ and $b \to \infty$. The system becomes

$$\begin{cases} \dot{q}_1 = -\dfrac{1}{\gamma}\partial_{q_1}\phi + \xi_{q_1}(t), \\ \dot{q}_2 = -\dfrac{1}{\gamma}\partial_{q_2}\phi + \xi_{q_2}(t), \end{cases} \tag{B1}$$

where the two equations are now decoupled. Thus, we only need to study the escape problem on the q_1-dimension. Then, the classical Kramers' formula[1,2] can be applied. For clarity, below we briefly review the derivation in our system.

The stationary probability current is

$$w \doteq -\Big[(\frac{1}{\gamma}\partial_{q_1}\phi)\rho + \frac{1}{\gamma}\epsilon\partial_{q_1}\rho\Big] = -\frac{1}{\gamma}\epsilon e^{-\phi/\epsilon}\partial_{q_1}(\rho e^{\phi/\epsilon}). \tag{B2}$$

It can be rewritten as

$$w e^{\phi/\epsilon} = -\frac{1}{\gamma}\epsilon\partial_{q_1}(\rho e^{\phi/\epsilon}). \tag{B3}$$

We do integration between the two points on the q-coordinate around the well W_1 to the saddle point S and get

$$w\Big|_{W_1}^{S} = -\frac{1}{\gamma}\epsilon(\rho e^{\phi/\epsilon})\Big|_{W_1}^{S}\Big(\int_{W_1}^{S} dq_1 e^{\phi/\epsilon}\Big)^{-1}. \tag{B4}$$

We assume that in a quasi-stationary state no particle has practically arrived at S. Also, near W_1, thermal equilibrium has practically been established. Thus we have

$$w\Big|_{W_1}^{S} = \frac{1}{\gamma}\epsilon\rho_{W_1}\Big(\int_{W_1}^{S} dq_1 e^{\phi/\epsilon}\Big)^{-1}, \tag{B5}$$

where $\rho_{W_1} \doteq (\rho e^{\phi/\epsilon})_{W_1}$.

We further assume that the potential function ϕ near W_1 can be approximated by a quadratic form and then the number n_{W_1} of particles near W_1 is

$$n_{W_1} = \int_{-\infty}^{+\infty} dq_1 \rho_{W_1} e^{-h^2(q_1+q^*)^2/2\epsilon} = \rho_{W_1}\sqrt{\frac{2\pi\epsilon}{h^2}}. \tag{B6}$$

The reaction velocity $r = w/n_{W_1}$, which denotes the chance in unit time that a particle starting from W_1 escapes to S. As a result, it is denoted by

$$r = \frac{w}{n_{W_1}} = \frac{1}{\gamma}\sqrt{\frac{h^2\epsilon}{2\pi}}\Big(\int_{W_1}^{S} dq_1 e^{\phi/\epsilon}\Big)^{-1}. \tag{B7}$$

For the potential barrier, we have the first order approximation

$$\begin{aligned} \int_{W_1}^{S} dq_1 e^{\phi/\epsilon} &= 2e^{\Delta E/\epsilon}\int_0^{+\infty} d(q_1 - q_S)e^{-h^2(q_S+q^*)(q_1-q_S)/\epsilon} \\ &= \frac{2\epsilon}{h^2(q_S+q^*)}e^{\Delta E/\epsilon} = \frac{2\epsilon}{h\sqrt{2\Delta E}}e^{\Delta E/\epsilon}, \end{aligned} \tag{B8}$$

where we have extended the upper limit of integration to $+\infty$ as larger values do not contribute to the integral.

Finally, the rate formula under the overdamped limit $\gamma \to \infty$ is

$$r = \frac{h^2}{\gamma}\sqrt{\frac{\Delta E}{4\pi\epsilon}}e^{-\Delta E/\epsilon}. \tag{B9}$$

This implies that the escape time goes to infinite when the friction coefficient becomes sufficiently large in Eq. (1). We have checked this rate formula for the overdamped limit by computer simulations as well (Fig. 2).

[1] H. A. Kramers, Physica **7**, 284 (1940).
[2] P. Hänggi, P. Talkner, and M. Borkovec, Rev. Mod. Phys. **62**, 251 (1990).
[3] A. Bray and A. McKane, Phys. Rev. Lett. **62**, 493 (1989).
[4] K. D. Duc, Z. Schuss, and D. Holcman, Phys. Rev. E **89**, 030101 (2014).
[5] M. F. Weber and E. Frey, Rep. Prog. Phys. **80**, 046601 (2017).
[6] H. Eyring, J. Chem. Phys. **3**, 107 (1935).
[7] F. Pinski and A. Stuart, J. Chem. Phys. **132**, 184104 (2010).
[8] M. Assaf, E. Roberts, Z. Luthey-Schulten, and N. Goldenfeld, Phys. Rev. Lett. **111**, 058102 (2013).
[9] S. Xu, S. Jiao, P. Jiang, and P. Ao, Phys. Rev. E **89**, 012724 (2014).
[10] J. H. Van't Hoff, *Etudes de Dynamique Chimique* (Muller, 1884), Vol. 1.
[11] S. Arrhenius, Z. Phys. Chem. **4**, 226 (1889) [English translation available in *Selected Readings in Chemical Kinetics*, edited by M. H. Back and K. J. Laidler (Elsevier, 1967), pp. 31–35].
[12] Y. Tang, R. Yuan, J. Chen, and P. Ao, Phys. Rev. E **91**, 042108 (2015).
[13] C. W. Gardiner, *Handbook of Stochastic Methods*, 3rd ed. (Springer-Verlag, Berlin, 2004).
[14] Y. Tang, R. Yuan, and P. Ao, Phys. Rev. E **92**, 062129 (2015).
[15] S. H. Strogatz, *Nonlinear Dynamics and Chaos: With Applications to Physics, Biology, Chemistry, and Engineering* (Westview Press, 2014).
[16] Y. Tang, R. Yuan, and Y. Ma, Phys. Rev. E **87**, 012708 (2013).
[17] R. S. Maier and D. L. Stein, Phys. Rev. E **48**, 931 (1993).
[18] F. Bouchet and J. Reygner, *Annales Henri Poincaré* (Springer, 2016), Vol. 17, pp. 3499–3532.
[19] J. Langer, Ann. Phys. **54**, 258 (1969).
[20] L. Yin and P. Ao, J. Phys. A: Math. Gen. **39**, 8593 (2006).

[21]X. Durang, C. Kwon, and H. Park, Phys. Rev. E **91**, 062118 (2015).
[22]B. Matkowsky, Z. Schuss, and E. Ben-Jacob, SIAM J. Appl. Math. **42**, 835 (1982).
[23]M. Borkovec and B. J. Berne, J. Chem. Phys. **82**, 794 (1985).
[24]R. Yuan and P. Ao, J. Stat. Mech. **2012**, P07010.
[25]P. Ao, J. Phys. A: Math. Gen. **37**, L25 (2004).
[26]H. Qian, Phys. Lett. A **378**, 609 (2014).
[27]N. Hashitsume, M. Toda, R. Kubo, and N. Saitō, *Statistical Physics II: Nonequilibrium Statistical Mechanics* (Springer, Berlin, 1991).
[28]Y. Tang, R. Yuan, and P. Ao, J. Chem. Phys. **141**, 044125 (2014).
[29]Y. Tang, R. Yuan, and P. Ao, Phys. Rev. E **89**, 062112 (2014).
[30]H. Risken, *The Fokker-Planck Equation: Methods of Solution and Applications* (Springer-Verlag, Berlin, 1984).
[31]R. Landauer, Phys. Rev. A **12**, 636 (1975).
[32]R. L. Liboff, Phys. Rev. **141**, 222 (1966).
[33]R. Czopnik and P. Garbaczewski, Phys. Rev. E **63**, 021105 (2001).
[34]G. Volpe, L. Helden, T. Brettschneider, J. Wehr, and C. Bechinger, Phys. Rev. Lett. **104**, 170602 (2010).
[35]A. Diehl and Y. Levin, J. Chem. Phys. **125**, 054902 (2006).
[36]V. Lisy and J. Tothova, Transp. Theory Stat. Phys. **42**, 365 (2013).
[37]D. P. Herzog, S. Hottovy, and G. Volpe, J. Stat. Phys. **163**, 659 (2016).
[38]G. Volpe and J. Wehr, Rep. Prog. Phys. **79**, 053901 (2016).
[39]I. Klik and L. Gunther, J. Stat. Phys. **60**, 473 (1990).
[40]W. T. Coffey, Y. P. Kalmykov, and S. V. Titov, Phys. Rev. B **89**, 054408 (2014).
[41]W. T. Coffey, D. S. F. Crothers, J. L. Dormann, Y. P. Kalmykov, E. C. Kennedy, and W. Wernsdorfer, Phys. Rev. Lett. **80**, 5655 (1998).
[42]M. C. Hickey and J. S. Moodera, Phys. Rev. Lett. **102**, 137601 (2009).
[43]M. Assaf and B. Meerson, Phys. Rev. E **81**, 021116 (2010).
[44]P. Talkner, Z. Phys. B: Condens. Matter **68**, 201 (1987).
[45]M. V. Day, Stochastics **20**, 121 (1987).
[46]M. Dykman, P. V. McClintock, V. Smelyanski, N. Stein, and N. Stocks, Phys. Rev. Lett. **68**, 2718 (1992).
[47]M. I. Dykman, M. M. Millonas, and V. N. Smelyanskiy, Phys. Lett. A **195**, 53 (1994).
[48]R. S. Maier and D. L. Stein, Phys. Rev. Lett. **71**, 1783 (1993).
[49]R. S. Maier and D. L. Stein, J. Stat. Phys. **83**, 291 (1996).
[50]Y. Tang, R. Yuan, G. Wang, X. Zhu, and P. Ao, Sci. Rep. **7**, 15762 (2017).
[51]R. Yuan, Y. Tang, and P. Ao, Front. Phys. **12**, 120201 (2017).